Allosteric Changes in Solvent Accessibility Observed in Thrombin upon Active Site Occupation†

Carrie Hughes Croy, Julia R. Koeppe, Simon Bergqvist, and Elizabeth A. Komives*

Department of Chemistry and Biochemistry, University of California, San Diego, 9500 Gilman Drive, La Jolla, California 92093-0378

Received January 4, 2004; Revised Manuscript Received March 3, 2004

ABSTRACT: The solvent accessibility of thrombin in its substrate-free and substrate-bound forms has been compared by amide hydrogen/deuterium ($H/^2H$) exchange. The optimized inhibitor peptide DPhe-Pro-Arg chloromethyl ketone (PPACK) was used to simulate the substrate-bound form of thrombin. These studies were motivated by the lack of observed changes in the active site of thrombin in the crystal structure of the thrombin−thrombomodulin complex. This result appeared to contradict amide exchange studies on the thrombin−thrombomodulin complex that suggested subtle changes occur in the active site loops upon thrombomodulin binding. Our results show that two active site loops, residues 214−222 and residues 126−132, undergo decreases in solvent accessibility due to steric contacts with PPACK substrate. However, we also observe two regions outside the active site undergoing solvent protection upon substrate binding. The first region corresponds to anion binding exosite 1, and the second is a β-strand-containing loop which runs through the core of the molecule and contains Trp141 which makes critical contacts with anion binding exosite 1. These results indicate two pathways of allosteric change that connect the active site to the distal anion binding exosite 1.

Thrombin is a multifunctional serine protease that plays a central role in regulating the blood clotting cascade. Like many of the other coagulation factors, a zymogen form of the protein exists as a mechanism of regulation required for normal hemostasis. The plasma concentration of prothrombin is estimated at 1.2 μM, but the plasma concentration of active thrombin does not exceed 0.06−0.09 μM (*1*). Thrombin plays both procoagulant and anticoagulant roles in the blood clotting cascade. When the clotting cascade is triggered, factor Xa must cleave prothrombin at two sites to result in the active α-thrombin protease. As an active protease its procoagulant function is to initiate the final step of the blood clotting cascade, cleavage of fibrinogen. Thrombin converts the soluble fibrinogen protein into an insoluble fibrin aggregate by cleaving the amino-terminal ends of the Aα and Bβ chains of fibrinogen which can then undergo polymerization and culminate in fibrin clot formation. Thrombin further amplifies procoagulant activity by also catalyzing activation of blood factors V, VII, VIII, and IX.

The procoagulation activities of α-thrombin are quickly diminished either as a result of capture by the endothially bound protein, thrombomodulin (TM),[1] or as a result of inhibition by antithrombin III. TM binding alters the substrate specificity of thrombin from fibrinogen to protein C, initiating anticoagulant function. The rate of protein C activation by thrombin is enhanced 20000-fold upon binding of TM and calcium ions (*2*, *3*). Protein C activation leads to the degradation of activated factors V and VIII and results in the shut down of the coagulation cascade (*4*). The switch in specificity of thrombin is a key component of natural hemostasis as unchecked procoagulation results in massive thrombi formation (*5*).

Thrombin has evolved to have high specificity for its substrates. Aspartate 235 ($D189_{CT}$)[2] at the bottom of the S1 site allows for substrate specificity of arginine and lysine residues at the P1 site (*6*). In general, thrombin prefers a hydrophobic residue, at the P2 site (Table 1) (*7*). The specificity of thrombin is also increased by the presence of extra insertion loops which restrict access into the active site. A substrate must be able to fit and interact with both of the active site insertion loops including residues 81−89 (the $60s_{CT}$ insertion loop) and the loop containing Leu132 ($Leu99_{CT}$) (*8*−*10*).

A number of studies have tried to address not only the elements that confer substrate specificity but the elements which switch specificity from procoagulant to anticoagulant. Crystal structures have helped to map contact regions between thrombin and TM, hirudin, fibrinopeptides, and small active site inhibitors such as DPhe-Pro-Arg chloro-

† This work was supported by NIH Grant RO1-HL070999.

* To whom correspondence should be addressed. Phone: (858) 534-3058. Fax: (858) 534-6174. E-mail: ekomives@ucsd.edu.

[1] Abbreviations: ABE1, anion binding exosite 1; TM, thrombomodulin; EGF, epidermal growth factor; TMEGF456, the fragment of TM containing the fourth, fifth, and sixth EGF-like domains; TFA, trifluoroacetic acid.

[2] Thrombin residues are conventionally numbered according to an alignment with chymotrypsin, and this convention results in loop residues carrying numbers such as 60A, 60B, etc. This convention is confusing with amide exchange data since information is lost regarding the length of the peptide fragment in which amide exchange is being measured. We therefore will give all thrombin residue information as sequential numbers first, followed, in parentheses, by the chymotrypsin convention numbers subscripted with CT to denote which are which.

10.1021/bi0499718 CCC: $27.50
Published on Web 04/10/2004

Table 1: Amino Acid Alignment for Naturally Occurring Substrates of Thrombin[a]

substrate	P9[b]	P8	P7	P6	P5	P4	P3	P2	P1	P1′	P2′	P3′	P4′
PPACK							DPhe	Pro	Arg				
fibrinogen													
human (Aα)	Phe	Leu	Ala	Glu	Gly	Gly	Gly	Val	Arg	Gly	Pro	Arg	Val
bovine (Aα)	Phe	Leu	Thr	Glu	Gly	Gly	Gly	Val	Arg	Gly	Pro	Arg	Val
human (Bβ)	Asn	Glu	Glu	Gly	Phe	Phe	Ser	Ala	Arg	Gly	His	Arg	Pro
antithrombin III													
human	Ser	Thr	Ala	Val	Val	Ile	Ala	Gly	Arg	Ser	Leu	Asn	Pro
bovine									Arg	Ser	Leu	Asn	Ser
protein C													
human	Asp	Gln	Glu	Asp	Gln	Val	Asp	Pro	Arg	Leu	Ile	Asp	Gly
bovine	Asp	Gln	Lys	Asp	Gln	Leu	Asp	Pro	Arg	Ile	Val	Asp	Gly

[a] Sequences were obtained from searching the gene databank at NCBI and from the CRC publication edited by Machovich (*1*). [b] P*x* denotes the number of positions the residue precedes the Arg cleavage residue (P1). P*x*′ denotes the number of positions the residue comes after the Arg cleavage residue.

methyl ketone (PPACK) (*8*−*12*). Mutagenesis experiments have aided the assignment of the roles of certain residues in binding versus catalysis (*7*, *13*−*16*). Arg217 ($Arg173_{CT}$) was studied in an alanine scan. This residue interacts with the fibrinopeptide and shows hydrogen bond contacts in the crystal structure but turns out to have minimal contribution to K_m (*7*, *8*). Trp263 ($Trp215_{CT}$) and Glu265 ($Glu217_{CT}$) have been shown to be important for procoagulant activity, and double mutation of these residues reduces the clotting rate by 20000-fold. These residues interact with the phenyl group at the P9 position of the fibrinogen substrate, and therefore, mutation of these residues has no effect on protein C since there is no aromatic residue in an equivalent position. Residues 177−190 ($W141_{CT}$−$K154_{CT}$) are called the autolysis loop because proteolytic cleavage within this loop compromises protein C activation and fibrinogen cleavage but has no affect on TM binding. Finally, mutations in other surface loops such as Arg233 ($Arg187_{CT}$), Glu265 ($Glu217_{CT}$), Cys267 ($C219_{CT}$), and Arg269−Lys272 (Arg 221_{CT}−Lys 224_{CT}) elicit an overall anticoagulant effect by lowering k_{cat} toward fibrinogen without effecting the k_{cat} for protein C (*7*, *17*). Thus, thrombin recognizes its multiple substrates by also using amino acids at remote sites on the protein surface.

Evidence is also building that binding to the remote anion binding exosite 1 (ABE1) may affect substrate specificity and/or catalytic rates. The substrate, fibrinogen, binds to both the active site and the ABE1 site of thrombin. TM also binds at the ABE1 site, and TM-bound thrombin shows remarkably different binding properties toward various inhibitors (*18*−*20*). Does thrombin use this site simply as a docking site to preorient fibrinogen toward the active site, or can it also utilize this region as a site that can propagate changes to other regions of the protease and prepare the active site for catalysis? The Fuentes-Prior crystal structure of thrombin−TMEGF456 suggests that thrombin does not undergo significant conformational changes upon cofactor binding (*11*). However, Parry et al. and Ye et al. showed that the fluorescence of PPACK analogues changed upon binding at ABE1 (*21*, *22*). Later, we also showed that TM binding caused changes in amide exchange of surface loops near the thrombin active site (*23*). In this study, we used amide $H/^2H$ exchange experiments to probe for differences in exchange between substrate-bound and substrate-free thrombin. Upon active site occupation by the optimized small peptide inhibitor, PPACK, changes in several surface loops including ABE1 were indeed observed.

MATERIALS AND METHODS

Proteins. Bovine thrombin was purified from a barium citrate eluate (prepared from bovine plasma) according to previously published methods (*24*). The eluate powder was redissolved overnight in 200 mL of 100 mM EDTA, 150 mM NaCl, and 10 mM sodium citrate, containing 11.8 g of ammonium sulfate and 0.03 g of benzamidine. The supernatant from a 35% ammonium sulfate cut was brought to 70% ammonium sulfate, and the pellet, containing prothrombin, was collected. After resuspension in 25 mL of 25 mM Tris, pH 7.5, and 100 mM NaCl, the prothrombin was desalted on a Sephadex G-25 gel filtration column (2.5 × 100 cm) and activated with 2.0 mg/mL *Echis carinatus* venom, 10 mM $CaCl_2$, and 1 mg/mL PEG-8000 for 60 min at 37 °C. After buffer exchange on a second G-25 column, the fraction containing active thrombin was loaded onto a MonoS FPLC column, 16/10 (Amersham-Pharmacia), equilibrated with buffer A (25 mM potassium phosphate, pH 6.5, 100 mM NaCl). The thrombin was eluted with a NaCl gradient to 500 mM NaCl over 1 h. α-Thrombin was identified by fibrinogen clotting assay, and the protein concentration was determined by absorbance at 280 nm (ϵ = 1.92 cm mL $unit^{-1}$ mg^{-1}).

Human thrombin was obtained from purified prothrombin (Haematologic Technologies). Optimal yields were obtained when the prothrombin concentrate was dissolved in 50 mM Tris, pH 7.5, 150 mM NaCl, 10 mM $CaCl_2$, and 0.1% PEG-8000 so that the final prothrombin concentration was 1.6 mg/mL. The prothrombin was then activated for 2 h at 37 °C and purified as above.

Portions of freshly purified human and bovine thrombin were incubated with a 30-fold molar excess of DPhe-Pro-Arg chloromethyl ketone (PPACK) (Bachem). After a 2 h incubation at room temperature, the PPACK-bound thrombin was repurified on a MonoS column as above. The PPACK-bound thrombin was devoid of fibrinogen clotting activity as expected.

For the mass spectrometry experiments, thrombin was buffer-exchanged so that during the amide $H/^2H$ exchange period the buffer concentration would be 25 mM KH_2PO_4, pH 6.5, and 50 mM NaCl. The human protein was not stable at high concentrations, so the two proteins were prepared in different manners. The human protein was exchanged into 12.5 mM KH_2PO_4, pH 6.5, and 25 mM NaCl and concentrated to ~1 mg/mL. Aliquots of 750 pmol of protein were

lyophilized and stored at −80 °C until use. The bovine thrombin was concentrated to 1 mg/mL, buffer-exchanged into 330 mM KH_2PO_4, pH 6.5, and 660 mM NaCl, concentrated to 4.5 mg/mL (122 μM), and then stored at −80° C until use.

Differential Scanning Calorimetry. DSC scans were collected using a MicroCal VP DSC instrument (MicroCal, Inc., Northampton, MA), using a protein concentration of 25−30 μM (∼1 mg/mL) thrombin. The temperature range scanned was 25−90 °C with a scan rate of 90 °C/h. Samples of thrombin were prepared in 25 mM PIPES, pH 6.5, and 150 mM NaCl.

Mass Spectrometry. Matrix-assisted laser desorption ionization time-of-flight (MALDI-TOF) mass spectra were acquired on a Voyager DE-STR instrument (Applied Biosystems) as previously described (*25*). The matrix used was 5.0 mg/mL α-cyano-4-hydroxycinnamic acid (Sigma-Aldrich) dissolved in a solution containing a 1:1:1 mixture of acetonitrile, ethanol, and 0.1% TFA. The pH of the matrix was adjusted to 2.2 using 2% TFA.

Peptides produced by pepsin cleavage of human thrombin were identified previously (*26*). Bovine thrombin peptides were identified by a combination of sequence searching for accurate masses, post-source decay sequencing, and MS/MS sequencing on a QSTAR ESI Q-TOF mass spectrometer. To carry out the digests, thrombin was brought to pH 2.2 in a 0.1% TFA solution and then incubated with a 2-fold molar excess of immobilized pepsin (Pierce Chemical Co.) for 10 min at 4 °C. There were no differences observed between the free and PPACK-bound forms of thrombin. The monoisotopic mass (MH^+) of all peptides identified was within 20 ppm of theoretical masses reported.

Amide H/^{2}H Exchange Experiments. The pH conditions during various stages of the reaction were determined on an Accumet Inlab 423 pH electrode (Mettler-Toledo) using nondeuterated mock solutions (to avoid having to recalibrate the electrode for deuterons). Experiments to measure amide exchange in human thrombin samples were performed as previously described (*23*, *26*). Briefly, exchange was initiated when a 750 pmol thrombin aliquot was resuspended in 12 μL of D_2O. The protein was allowed to exchange (pD* 6.5, not corrected) at room temperature for 1−10 min. The exchange was quenched by a 10-fold dilution into a prechilled vial (0 °C) containing a quench buffer composed of water and 2% TFA, making the final solution approximately 0.1% TFA, pH 2.2. The quenched protein was then digested as described above. The digest was aliquoted into several fractions, rapidly frozen in liquid N_2, and stored at −80 °C.

Experiments to measure amide exchange in bovine thrombin by quench flow were carried out using a Kin-Tek RQF-3 flow-quench apparatus (Kin-Tek Corp., Clarence, PA). The deuteration was initiated when 19 μL of a 122 μM bovine thrombin solution (2.3 nmol) was diluted 13.8-fold into D_2O (203 μL) at room temperature for 0.05, 0.5, 5, 50, and 120 s. After the exchange period, the reaction was quenched by a 6-fold dilution into a prechilled vial (0 °C) containing 1190 μL of a quench buffer composed of water and 2% TFA, making the final solution approximately 0.1% TFA, pH 2.2, containing 0.7 pmol/μL bovine thrombin. We did not use the third "quench" syringe because we needed to maintain the same volume of final quenched solution. The quenched protein then was digested as described above. The digest was aliquoted into several fractions, rapidly frozen in liquid N_2, and stored at −80 °C.

Samples were analyzed by MALDI-TOF mass spectrometry one at a time to minimize off-exchange. Samples were rapidly thawed, mixed with cold matrix, spotted on a prechilled MALDI target plate, and dried under vacuum (*23*). The mass spectra were analyzed to determine the average number of deuterons present in each peptic peptide. The number of deuterons incorporated in each peptide was quantified by subtracting the centroid of the undeuterated control from the centroid of the isotopic peak cluster for the deuterated sample. All values reported represent only the deuterons exchanged onto the backbone amide−hydrogen (NH) positions. The residual deuterium content (9% for bovine and 5% for human) that incorporated into rapidly exchanging side chain positions was subtracted. Finally, data were corrected for back-exchange loss (∼45% for both species) as described previously (*23*, *26*, *27*).

RESULTS

Thrombins from Two Species Were Used. Over many years, the similarity of both sequence and activity of thrombins from various species has been noted. Our laboratory has demonstrated that the kinetics and thermodynamics of the interaction between thrombin and thrombomodulin for both species are indistinguishable (*28*). In the study presented here, we used both species in order to compare and contrast the results from these two similar proteins. Peptic cleavage of bovine thrombin resulted in 25 peptides which were identified by various MS/MS sequencing techniques (Figure 1A). Quantitative data were obtained for 16 of these peptides and resulted in coverage of 38% of the primary sequence (Figure 1C). The regions of bovine thrombin represented by quantifiable digest products were not identical to those obtained by experiments on human thrombin (*23*, *26*). Digestion of human thrombin yielded additional coverage in regions such as the light chain and C-terminus of the protein (Figure 1B,C). Final sequence coverage when the data from both species were combined was 50% (Figure 1C).

Amide H/^{2}H Exchange Experiments. Amide H/^{2}H exchange experiments were designed to probe the solvent accessibility of regions of thrombin and to assess which regions of the protein undergo changes in solvent accessibility upon active site occupation. PPACK, an optimized thrombin inhibitor, was used to simulate a substrate-bound state (*9*). Initial amide H/^{2}H exchange experiments using exchange periods of 1, 2, 5, and 10 min revealed that several surface loops including the TM-binding loop at ABE1 exchanged fully within the first 5 min. A series of quench-flow experiments were, therefore, used to capture shorter deuteration times. The deuteration periods for the quench flow were 50 ms to 2 min.

Figure 2 shows how the peak envelope of a peptide shifts to higher mass as more labile amide positions exchange over time. Since the labeling occurs when the protein is in its native ensemble of states, the amount of deuteration reflects the solvent accessibility of the protein region. To determine which regions of thrombin show altered solvent accessibility due to the presence of a substrate in the active site, the deuteration levels of the substrate-free protein were compared to that of the PPACK-bound protein.

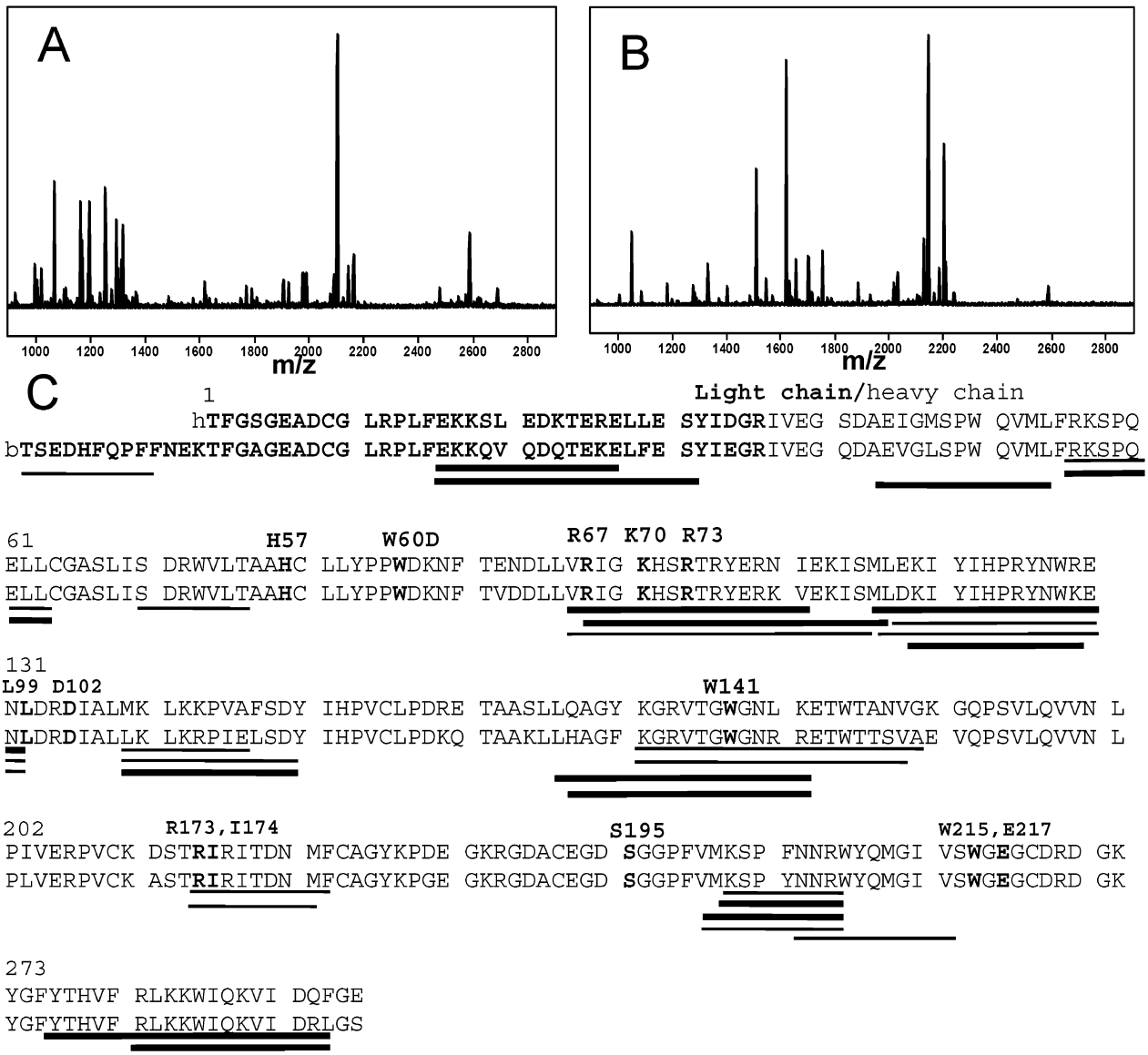

FIGURE 1: (A) MALDI-TOF mass spectrum of bovine thrombin after peptic digestion. From this mass spectrum, a total of 24 peptides were identified via MS/MS sequencing. (B) MALDI-TOF mass spectrum of human thrombin after peptic digestion. A total of 25 peptides were identified as previously described (*25*). (C) Aligned sequences of human and bovine α-thrombin showing all of the peptides generated by pepsin cleavage as lines below the sequence. Thick lines denote peptides from the human protein digest, and thin lines denote those from the bovine digest. The light chain residues of thrombin are indicated by bold type, and significant residues including the catalytic triad (H57, D102, and S195) are in both bold type and annotated above the sequence in the chymotrypsin numbering system. Coverage of the thrombin sequence is low, in part due to the four disulfide bonds present in thrombin.

Changes at the Active Site of Thrombin. Two loops surrounding the rim of the active site showed differences in deuterium incorporation between free and PPACK-bound forms of thrombin (Table 2, Figure 8). One region is represented by the bovine thrombin peptide containing residues 214−222 ($Arg173_{CT}$−$Phe181_{CT}$, peptide mass MH^+ 1165.62). It should be noted that this peptide did not show the high levels of deuterium incorporation expected for a completely accessible surface loop. Also, the mass spectra of this peptide reveal that, even at short deuteration periods, PPACK-bound thrombin incorporated one less deuteron than free thrombin (Figure 3A). This difference is constant throughout exchange (Figure 3B) and remains even at an exchange period of 120 min (data not shown). The structures of PPACK-bound and fibrinopeptide A-bound human thrombin reveal that the difference may arise because of the close proximity of Ile215 ($Ile174_{CT}$) to the phenylalanine ring of the PPACK or fibrinopeptide A (*8*−*10*). This is one of five residues that helps to form a hydrophobic pocket for the phenyl ring. The preceding Arg214 ($Arg173_{CT}$) also forms a hydrogen bond when the active site is occupied by fibrinopeptide A (*8*, *9*). These two findings support that this active site loop undergoes changes either in dynamics or in solvent accessibility upon substrate binding, and these changes can be observed by amide $H/^2H$ exchange methods.

A second active site region that showed differences between substrate-free and -bound thrombin was the peptide spanning residues 117−132 ($90s_{CT}$ insertion loop). The bovine protein had peptide MH^+ 2102.12, residues 117−132, and the human protein had two peptides, MH^+ 2144.14, residues 117−132, and MH^+ 1331.75, residues 117−126. The mass spectra of the 117−132 peptides from the two species are shown in Figure 4A,B and the kinetic plots of deuteration in Figure 4C,D. For both species, this region of

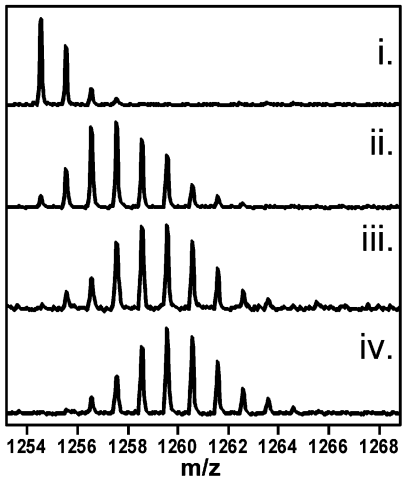

FIGURE 2: Region of the MALDI-TOF mass spectrum showing the peptide at MH^+ 1254.54 from the peptic digest of bovine thrombin. (i) The peptide before deuteration. The peaks of higher mass in the undeuterated peptide envelope are caused by the presence of naturally occurring isotopes. (ii) The peptide after deuteration for 50 ms. (iii) The peptide after deuteration for 5 s. (iv) The peptide after deuteration for 50 s. The peaks of higher mass in the deuterated peptide envelopes are caused by a convolution of amide exchange and the presence of naturally occurring isotopes. To quantitate the number of deuterons incorporated in each peptide, the centroid of the undeuterated control was subtracted from the centroid of the isotopic peak cluster for the deuterated sample.

Table 2: Quantitative Analysis of Peptic Fragments of Thrombin

region of thrombin[a]	no. of NH	no. of deuterons active[b]	no. of deuterons PPACK[b]
−13 to −4 (B, 1254.54)	8	7.4 ± 0.2	7.5 ± 0.1
54−61 (B, 1004.55)	6	3.4 ± 0.2	3.3 ± 0.2
68−74 (B, 888.49)	6	0.7 ± 0.1	0.6 ± 0.1
96−116 (B, 2586.48)	20	17.8 ± 0.3	16.2 ± 0.3
117−132 (B, 2102.12)	14	8.2 ± 0.2	6.5 ± 0.1
138−149 (B, 1311.80)	9	4.2 ± 0.2	4.0 ± 0.1
139−146 (B, 996.66)	6	2.5 ± 0.1	2.5 ± 0.1
171−189 (B, 2162.12)	18	11.7 ± 0.4	8.4 ± 0.3
214−222 (B, 1165.62)	8	3.5 ± 0.2	2.5 ± 0.3
248−255 (B, 1064.53)	6	3.4 ± 0.2	3.5 ± 0.1
252−262 (B, 1367.65)	10	3.7 ± 0.1	3.4 ± 0.1
11−16 (H, 1934.01)	15	1.4 ± nd	1.4 ± nd
43−54 (H, 1399.66)	10	4.6 ± 0.1	4.5 ± 0.1
96−112 (H, 2127.19)[c]	16	11.4 ± 0.1	10.8 ± 0.1
97−117 (H, 2586.44)	20	17.0 ± 0.1	16.0 ± 0.2
117−126 (H, 1331.75)[c]	8	1.6 ± 0.1	1.7 ± 0.1
117−132 (H, 2144.14)	14	6.9 ± 0.2	5.4 ± 0.2
166−180 (H, 1619.87)	14	5.2 ± 0.2	2.8 ± 0.1
247−255 (H, 1179.57)	7	4.1 ± 0.1	4.1 ± 0.1
276−292 (H, 2202.26)	16	5.4 ± 0.2	5.5 ± 0.2
281−293 (H, 1702.02)	12	4.1 ± 0.1	4.1 ± 0.1

[a] Overlapping peptides of thrombin that only differed by one amino acid (see Figure 1C) are not reported in this table. [b] All values have been corrected for losses due to back-exchange (45%), and errors are the standard deviation of the mean of two independent experiments. The values reported for the bovine data were after 50 s of exchange and for the human were after 60 s. [c] This value does not reflect the total number of deuterons incorporated into this peptide because the area of integration had to be truncated due to the presence of an interfering peak at higher mass.

free thrombin incorporated approximately 1.5 more deuterons than the PPACK-bound thrombin (Table 2, Figure 8). The digest of the human protein produced a second overlapping peptide covering residues 117−126 (MH^+ 1331.75). This peptide showed no differences in the free vs PPACK-bound

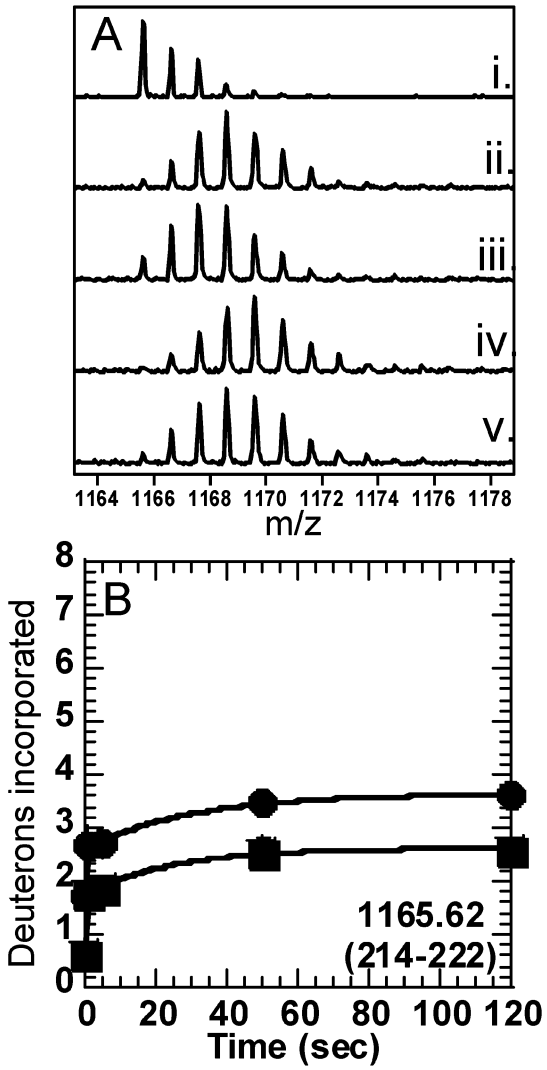

FIGURE 3: (A) Region of the MALDI-TOF mass spectrum showing the peptide at MH^+ 1165.62 from the peptic digest of bovine thrombin. (i) The peptide before deuteration. (ii) The peptide after the free thrombin deuterated for 50 ms. (iii) The peptide from the PPACK-bound thrombin deuterated for 50 ms. (iv) The peptide after the free thrombin deuterated for 50 s. (v) The peptide from the PPACK-bound thrombin deuterated for 120 s. (B) Kinetic plot of the amide $H/^2H$ exchange data obtained for the MH^+ 1165.62 peptide from the free (●) and PPACK-bound (■) forms of thrombin.

protein (Figure 4E), allowing us to narrow down the region of differences to residues 127−132 ($Arg97_{CT}$−$Leu99_{CT}$), also known as the 90s insertion loop. This loop is located at the mouth of the active site, and crystal structures of fibrinopeptide A-bound protein reveal that residues Arg128 ($Arg97_{CT}$) and Glu129 ($Glu97A_{CT}$) are critical for orienting fibrinopeptide A into the active site (*8*, *9*). In addition, the function of Leu132 ($Leu99_{CT}$) is to form another part of the hydrophobic pocket for the phenylalanine ring of PPACK.

Changes Far from the Active Site of Thrombin. Two regions of thrombin showed differences that could not be attributed to contacts with the PPACK molecule. The first region is the autolysis loop represented by two overlapping peptides covering residues 166−189 ($Leu130_{CT}$−$Gly149D_{CT}$). The peptide of mass MH^+ 1619.87 in the human protein covers residues 166−180 ($Leu130_{CT}$−$Leu143_{CT}$) (Figure 5A) and showed a difference of 2.4 deuterons between the two states of thrombin (Table 2, Figures 5B and 8). The peptide

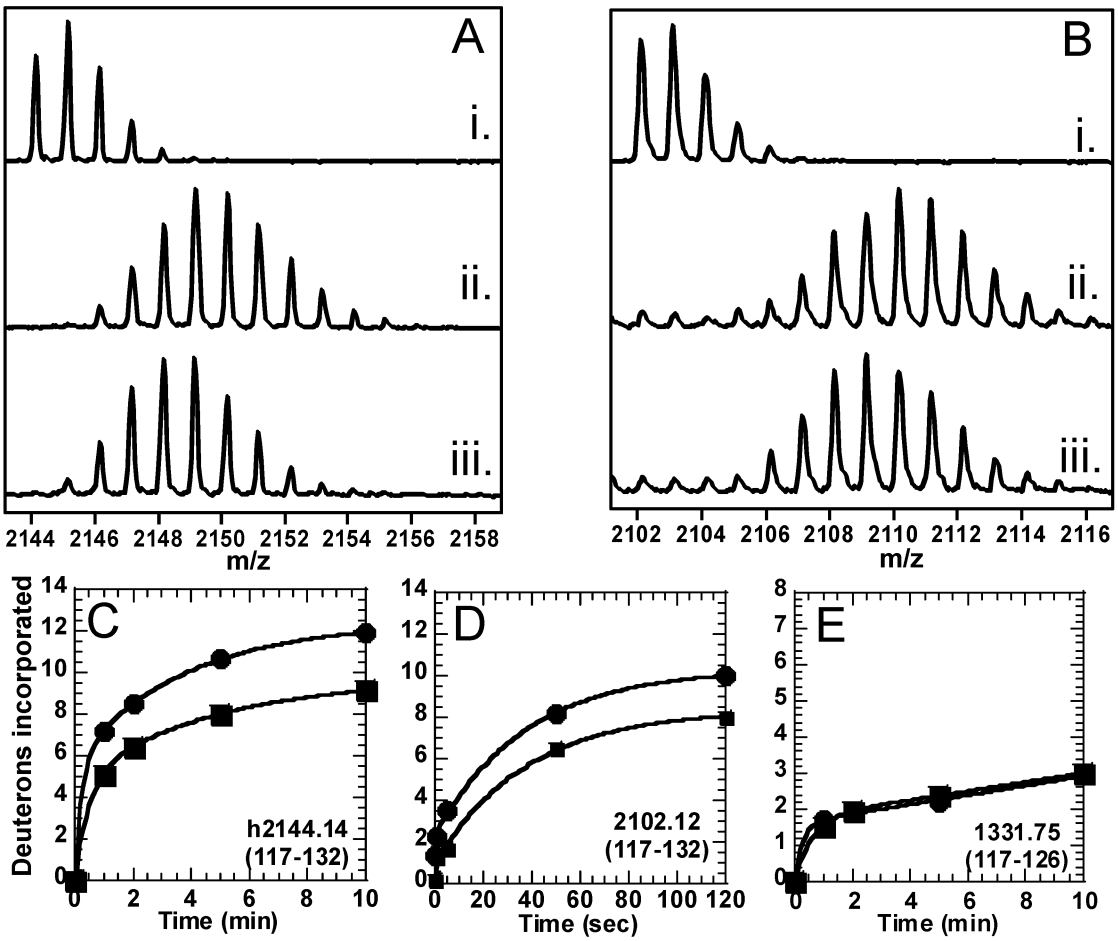

FIGURE 4: (A) Region of the MALDI-TOF mass spectrum showing the peptide at MH^+ 2144.14 from the peptic digest of human thrombin. (i) The peptide before deuteration. (ii) The peptide from free thrombin after deuteration for 120 s. (iii) The peptide from PPACK-bound thrombin after deuteration for 120 s. (B) Region of the MALDI-TOF mass spectrum showing the peptide at MH^+ 2102.12 from the peptic digest of bovine thrombin. Spectra are the same as in (A). (C) Kinetic plot of the amide H/^{2}H exchange data obtained for the peptide at MH^+ 2144.14 from free (●) and PPACK-bound (■) forms of thrombin. (D) Kinetic plot of the H/^{2}H data obtained for the peptide at MH^+ 2102.12 peptide from free (●) and PPACK-bound (■) thrombin. (E) Kinetic plot of the amide H/^{2}H exchange data obtained for the peptide at MH^+ 1331.75 from free (●) and PPACK-bound (■) thrombin.

with MH^+ 2162.12 of the bovine protein covers residues 171−189 ($Lys135_{CT}$−$Gly149D_{CT}$) (Figure 5C) and showed a difference of 3.3 deuterons (Table 2, Figure 5D).

The final region of thrombin that showed alteration in solvent accessibility upon active site occupation was ABE1. This region of thrombin is the distal site of binding for fibrinogen, as well as other proteins that interact with thrombin. Three peptides covering residues 96−117 (66_{CT}−86_{CT}) were found to be highly solvent accessible. In fact, the region was found to be fully deuterated by 10 min in both species of thrombin. Both the human and bovine protein had a peptide of MH^+ 2586.44 although they corresponded to slightly different overlapping regions, 97−117 and 96−116, respectively. The mass spectra for the peptide from human thrombin, after a 60 s deuteration period, are shown in Figure 6A. The kinetic plots show that a small, but real difference in deuterium incorporation between the active and PPACK-bound thrombin is present between 1 and 5 min (Figure 6B). This difference completely disappears by 10 min because in both forms of thrombin this region was by then fully deuterated. These results are confirmed by a second shorter peptide representing residues 96−112 (66_{CT}−80_{CT}) (MH^+ 2127.19) in the human protein (Table 2, Figure 8).

Since this region exchanges so readily, we decided to look at the deuterium incorporation at shorter exchange periods using a quench-flow instrument. The human protein was not amenable to the conditions demanded by these experiments, so the results from only the bovine protein are presented here. The spectra in Figure 6C show the peptide of mass 2586.44 after a 5 s deuteration period. The kinetic plots of both the bovine and human data show that the differences between the two forms of the protein arise early and are occurring in a region of the protein which has little solvent protection (Figure 6B,D).

PPACK Induces Overall Tightening of Thrombin. The data summarized in Table 2 revealed that all regions of thrombin which experienced differences in amide exchange showed less solvent accessibility for the PPACK-bound form compared to the free form. Previous amide H/^{2}H exchange studies on PKA and MAP kinase showed that there was a mixture of regions which showed increases and decreases in amide exchange upon perturbation of the protein (*29*, *30*). To test whether the presence of the PPACK molecule was causing a global change in thrombin, we performed DSC to measure the overall thermostability of the two forms of bovine thrombin. The DSC thermogram showed that the PPACK-bound form of thrombin was significantly more stable; the

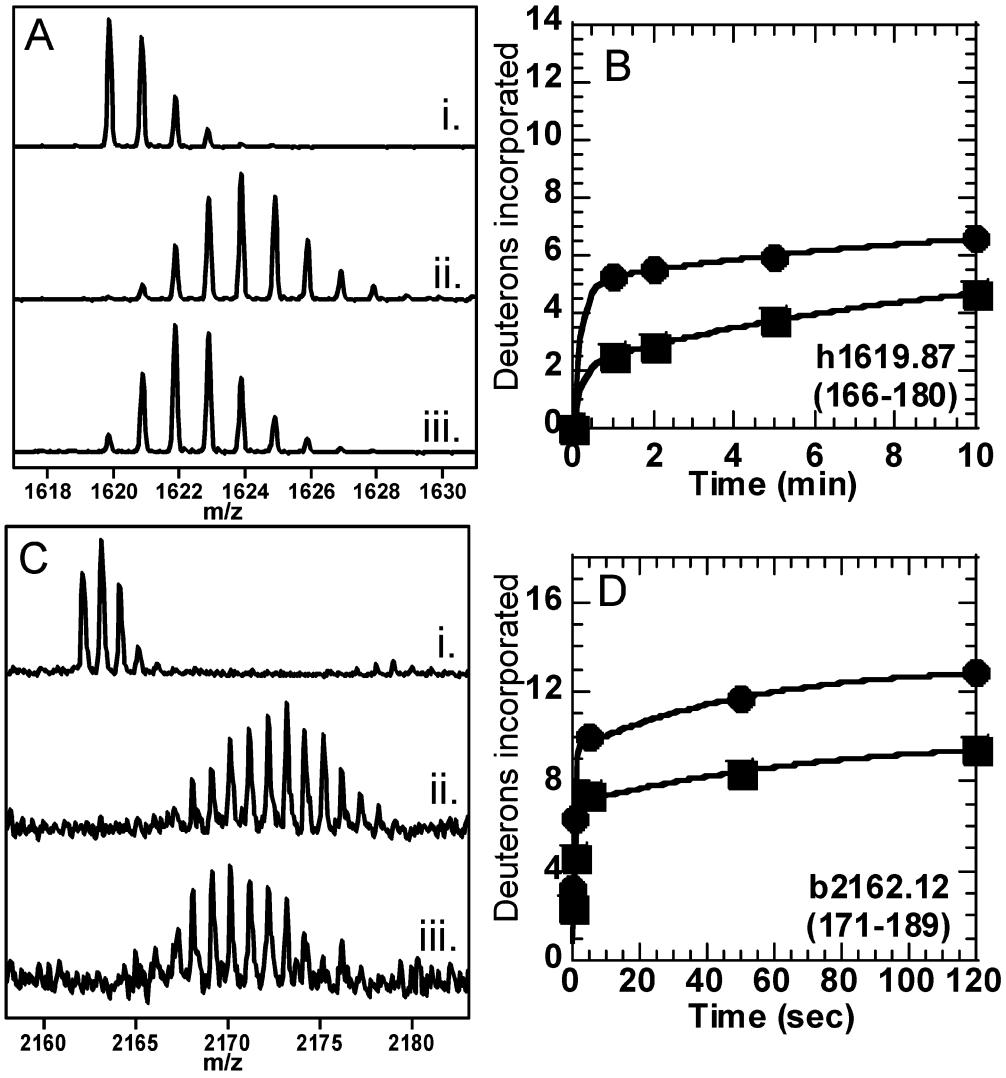

FIGURE 5: (A) Region of the MALDI-TOF mass spectrum showing the peptide at MH^+ 1619.87 from the peptic digest of human thrombin. (i) The peptide before deuteration. (ii) The peptide from free thrombin after deuteration for 50 s. (iii) The peptide from the PPACK-bound thrombin after deuteration for 50 s. (B) Kinetic plot of the amide H/^{2}H exchange data obtained for the peptide at MH^+ 1619.87 from free (●) and PPACK-bound (■) thrombin. (C) Region of the MALDI-TOF mass spectrum showing the peptide at MH^+ 2162.12 from the peptic digest of bovine thrombin. (i) The peptide before deuteration. (ii) The peptide from free thrombin after deuteration for 50 s. (iii) The peptide from the PPACK-bound thrombin after deuteration for 50 s. (D) Kinetic plot of the amide H/^{2}H exchange data obtained for the 2162.12 peptide from free (●) and PPACK-bound (■) thrombin.

temperature of unfolding for the PPACK protein was 79 °C vs the free form which was 57 °C (Figure 7). These results suggest that stabilization of the thrombin molecule occurs upon substrate binding. It is likely that the decrease in solvent accessibility of several surface loops is related to the increased stability of the substrate-bound form.

DISCUSSION

Changes in the Active Site Loops. The crystal structure of human thrombin cocrystallized with PPACK shows that two of the active site loops, the one containing Arg214 ($Arg173_{CT}$) and the one containing Leu132 ($Leu99_{CT}$), come in contact with the PPACK molecule (*10*). Both of these loops incorporated less deuterium when PPACK was present in the active site (Figure 8). Although the decreased deuterium incorporation into the backbone amides of these loops could be due to dynamic changes, the most likely explanation for the lower levels of amide exchange is simply steric contacts with the PPACK molecule. Two other regions of the thrombin molecule, the autolysis loop and the ABE1 loop, also showed lower levels of amide exchange in the PPACK-bound form of thrombin. These could *not* be attributed to contacts with the PPACK molecule and must reflect decreased dynamics of the loop or a restricted ensemble of conformations.

Lines of Communication between the Active Site and ABE1. ABE1 is a binding site for fibrinogen, TM, and hirudin. Hofsteenge illustrated the importance of this region by showing that proteolytic cleavage leading to the deletion of residues 99−109 ($Ile68_{CT}$−$Arg77A_{CT}$), and the formation of γ-thrombin, abolishes the binding of fibrinogen and TM (*31*). The crystal structure of the thrombin−TMEGF456 complex further showed that it was Arg104, Arg106, Arg109, Tyr107, and Ile114 ($Arg73_{CT}$, $Arg75_{CT}$, $Arg77A_{CT}$, $Tyr76_{CT}$, and $Ile82_{CT}$) that were interaction sites for TM binding (*11*). Indeed, amide exchange studies showed a decrease in exchange within residues 97−117 that could be attributed to solvent exclusion upon TM binding (*23*). Many of the

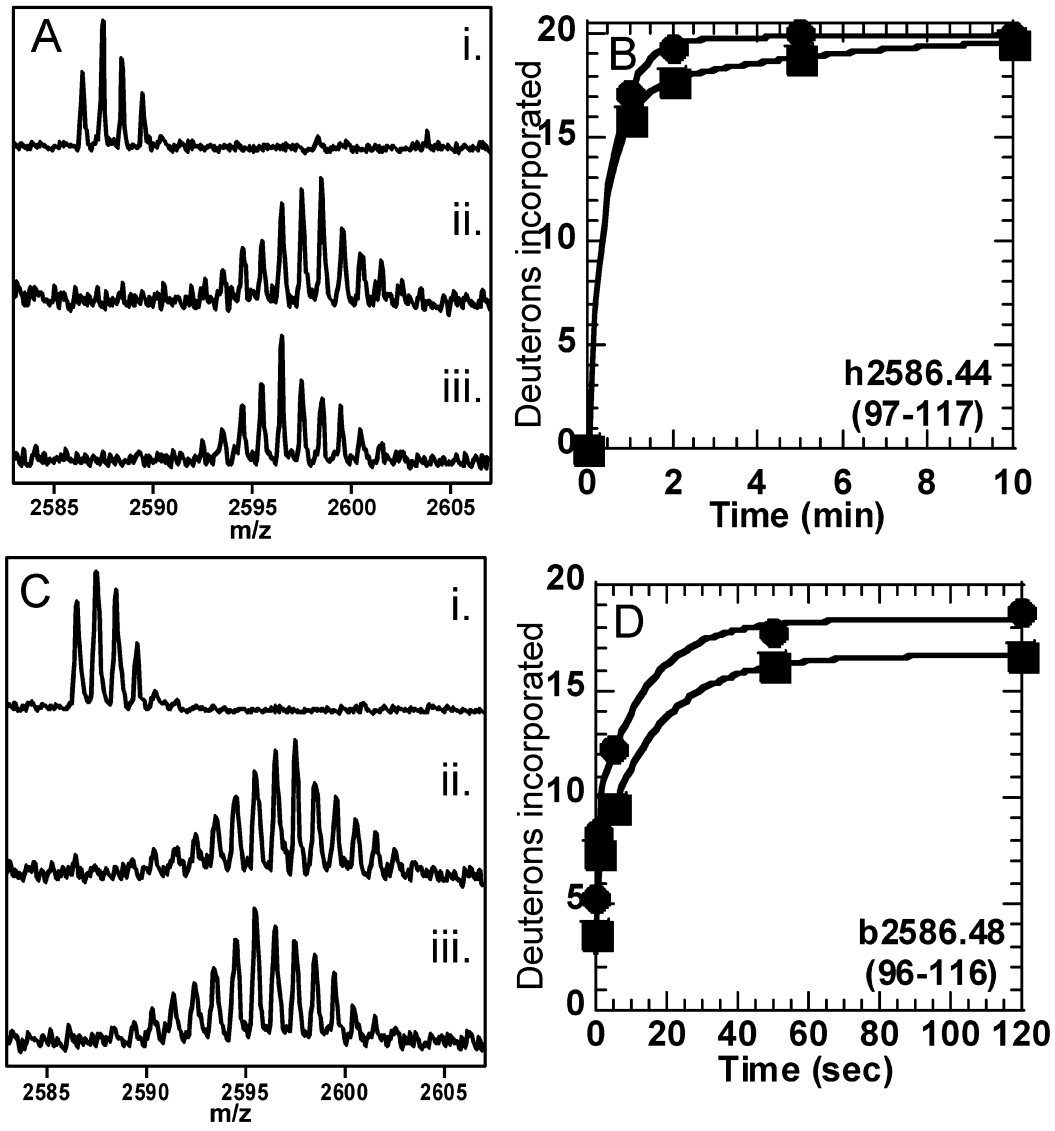

FIGURE 6: (A) Region of the MALDI-TOF mass spectrum showing the peptide at MH^+ 2586.44 from the peptic digest of human thrombin. (i) The peptide before deuteration. (ii) The peptide from free thrombin after deuteration for 50 s. (iii) The peptide from PPACK-bound thrombin after deuteration for 50 s. (B) Kinetic plot of the H/^{2}H data obtained for the peptide at MH^+ 2586.44 from free (●) and PPACK-bound (■) human thrombin. (C) Region of the MALDI-TOF mass spectrum showing the peptide at MH^+ 2586.48 from the peptic digest of bovine thrombin. (i) The peptide before deuteration. (ii) The peptide from free thrombin after deuteration for 50 s. (iii) The peptide from PPACK-bound thrombin after deuteration for 50 s. (D) Kinetic plot of the amide H/^{2}H exchange data obtained for the peptide at MH^+ 2586.48 from free (●) and PPACK-bound (■) bovine thrombin.

surface segments showed changes upon active site occupation, suggesting a dynamic communication between the TM-binding site, ABE1, and the active site (Table 3). The amide H/^{2}H exchange studies presented here allow us to elucidate two different pathways along which communication between the active site and ABE1 may occur.

An indirect line of communication could be traced from the active site to ABE1 (colored red) via the autolysis loop, residues 181−191 (145_{CT}−$149E_{CT}$, colored orange). Peptides corresponding to residues 166−180 and 171−189 became much less deuterated (2.4 and 3.3 deuterons, respectively) in the PPACK-bound thrombin. This loop and β-strand lie between the catalytic serine loop and ABE1 (Figure 8). The side chain of Trp177 ($Trp141_{CT}$) makes the final connection to ABE1, completing the path. The crystal structure of thrombin shows that the side chain of this tryptophan makes multiple contacts with the backbone of ABE1, specifically

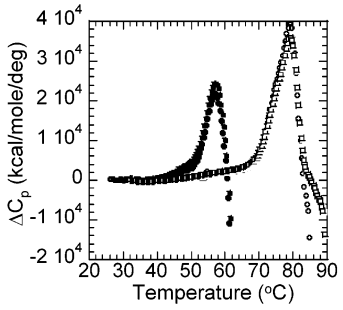

FIGURE 7: Differential scanning calorimetry was used to measure the thermal stability of bovine thrombin with the PPACK molecule bound at the active site (open symbols) and that without the PPACK molecule (closed symbols). The thermogram shows that the temperature of unfolding is 22 °C higher for the PPACK-bound form of thrombin (79 vs 57 °C). It should be noted that the curves were not reversible and indicate an aggregation event is occurring after the observed transition.

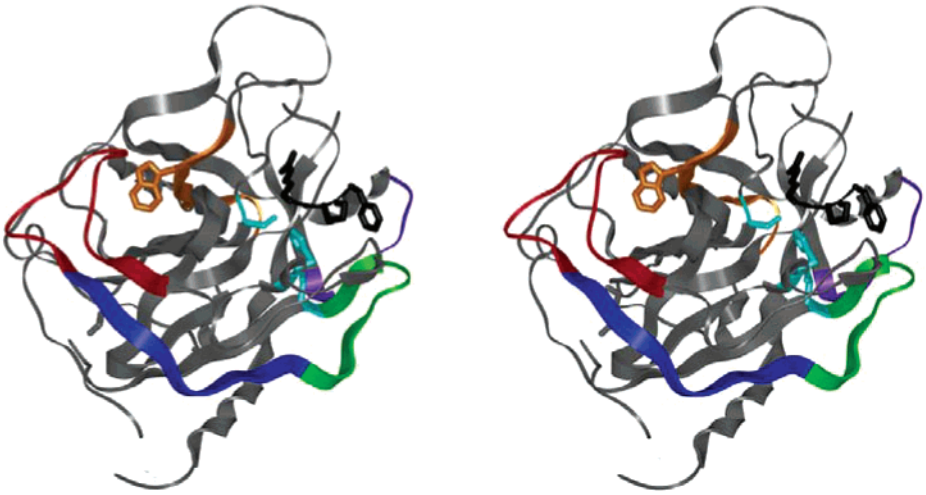

FIGURE 8: Stereoview of the structure of human α-thrombin (gray) with PPACK (black, stick model) bound at the active site (catalytic residues colored cyan). The four regions that are less solvent accessible in the PPACK-bound thrombin correspond to residues 214−222 (Arg173$_{CT}$−Phe181$_{CT}$, purple), residues 126−132 (the 90s$_{CT}$ loop, green), residues 97−117 (ABE1 residues Val66$_{CT}$−Glu85$_{CT}$, red), and residues 166−189 (the Trp141$_{CT}$ loop, orange). The surface β-strand that connects ABE1 to the 90s$_{CT}$ loop is colored blue.

Table 3: Summary of Changes Observed in Thrombin from Amide H/^{2}H Exchange Experiments[a]

thrombin region sequential numbering	changes observed upon TM binding	changes observed upon PPACK binding
ABE1 region		
A, 97−117	yes	yes
B, 97−112	yes	yes
C, 54−61	yes	no
peripheral sites to ABE1		
A, 139−149	yes	no
B, 167−180	yes	yes
C, 181−189	not observed	yes
D, 281−293	yes	no
E, 117−132	yes	yes

[a] Yes denotes regions of thrombin where the deuterium content differs between the free form of thrombin and the PPACK (this study) or TM [previous work (*23*)] bound thrombin. Differences are not quantified because the data were collected by two different types of H/^{2}H experimental methods (deuteron retention vs deuteron incorporation).

to residues His102−Arg104 (His71$_{CT}$−Arg73$_{CT}$). The conservation of Trp141$_{CT}$ throughout the thrombin family suggests that this pathway may be functionally relevant (*32*).

A second, direct line can be traced from the catalytic Asp135 (Asp102$_{CT}$) residue, through the active site loop containing residues 126−132 (90s$_{CT}$ insertion loop, colored green), to residues 97−117 (the ABE1 loop, residues Arg67$_{CT}$−Glu85$_{CT}$, colored red) (Figure 8). Thus, orientation of the 90s insertion loop upon contact with the substrate molecule may transmit changes from the active site down the surface β-strand (colored blue) to ABE1. It is interesting to note that this surface β-strand does not show differences in amide exchange between the PPACK-bound and free forms of thrombin (cf. Figure 4E). Thus, the connecting strand appears to function in a manner similar to the rope in a tug of war in that it remains taut but tugging on one end propagates changes at the other.

It is likely that *both* of the lines of communication from the active site to ABE1 are important for the multiple functions of thrombin. Mutagenesis of various residues along the communication lines coupled with amide exchange experiments will help to determine how each of them regulates the procoagulant and anticoagulant functions of this important protein.

REFERENCES

1. Machovich, R. (1984) *The Thrombins*, p 166, CRC Press, Boca Raton, FL.
2. Esmon, C. T., and Owen, W. G. (1981) Identification of an endothelial cell cofactor for thrombin-catalyzed activation of protein C, *Proc. Natl. Acad. Sci. U.S.A. 78*, 2249−2252.
3. Esmon, C. T. (2000) Regulation of blood coagulation, *Biochim. Biophys. Acta 1477*, 349−360.
4. Musci, G., Berliner, L. J., and Esmon, C. T. (1988) Evidence for multiple conformational changes in the active center of thrombin induced by complex formation with thrombomodulin: an analysis employing nitroxide spin-labels, *Biochemistry 27*, 769−773.
5. Griffin, J. H., Ecatt, B., Zimmerman, T. S., Kleiss, A. J., and Widerman, C. (1981) Deficiency of protein C in congenital thrombotic disease, *J. Clin. Invest. 68*, 1370−1373.
6. Vindigni, A., Dang, Q. D., and Di Cera, E. (1997) Site-specific dissection of substrate recognition by thrombin, *Nat. Biotechnol. 15*, 891−895.
7. Di Cera, E., and Cantwell, A. M. (2001) Determinants of thrombin specificity, *Ann. N.Y. Acad. Sci. 936*, 133−146.
8. Stubbs, M. T., Oschkinat, H., Mayr, I., Huber, R., Angliker, H., Stone, S. R., and Bode, W. (1992) The interaction of thrombin with fibrinogen. A structural basis for its specificity, *Eur. J. Biochem. 206*, 187−195.
9. Martin, P. D., Robertson, W., Turk, D., Huber, R., Bode, W., and Edwards, B. F. (1992) The structure of residues 7−16 of the A alpha-chain of human fibrinogen bound to bovine thrombin at 2.3-Å resolution, *J. Biol. Chem. 267*, 7911−7920.
10. Bode, W., Turk, D., and Karshikov, A. (1992) The refined 1.9-Å X-ray crystal structure of D-Phe-Pro-Arg chloromethylketone-inhibited human alpha-thrombin: structure analysis, overall structure, electrostatic properties, detailed active-site geometry, and structure−function relationships, *Protein Sci. 1*, 426−471.
11. Fuentes-Prior, P., Iwanaga, Y., Huber, R., Pagila, R., Rumennik, G., Seto, M., Morser, J., Light, D. R., and Bode, W. (2000) Structural basis for the anticoagulant activity of the thrombin-thrombomodulin complex, *Nature 404*, 518−525.
12. Grutter, M. G., Priestle, J. P., Rahuel, J., Grossenbacker, H., Bode, W., Hofsteenge, J., and Stone, S. R. (1990) Crystal structure of the thrombin-hirudin complex: a novel mode of serine protease inhibition, *EMBO J. 9*, 2361−2365.
13. Hall, S. W., Nagashima, M., Zhao, L., Morser, J., and Leung, L. L. K. (1999) Thrombin interacts with thrombomodulin, protein C, and thrombin-activatable fibrinolysis inhibitor via specific and distinct domains, *J. Biol. Chem. 274*, 25510−25516.

14. Tsiang, M., Jain, A. K., Dunn, K. E., Rojas, M. E., Leung, L. L. K., and Gibbs, C. S. (1995) Functional mapping of the surface residues of human thrombin, *J. Biol. Chem. 270*, 16854−16863.
15. Wu, Q., Picard, V., Aiach, M., and Sadler, J. E. (1994) Activation-induced exposure of the thrombin anion-binding exosite. Interactions of recombinant mutant prothrombins with thrombomodulin and a thrombin exosite-specific antibody, *J. Biol. Chem. 269*, 3725−3730.
16. Ayala, Y. M., Cantwell, A. M., Rose, T., Bush, L. A., Arosio, D., and Di Cera, E. (2001) Molecular Mapping of Thrombin-Receptor Interactions, *Proteins: Struct., Funct., Genet. 45*, 107−116.
17. Arosio, D., Ayala, Y. M., and Di Cera, E. (2000) Mutation of W215 compromises thrombin cleavage of fibrinogen, but not of PAR-1 or protein C, *Biochemistry 39*, 8095−8101.
18. Myles, T., Church, F., Whinna, H., Monard, D., and Stone, S. R. (1998) Role of thrombin anion-binding exosite-I in the formation of thrombin-serpin complexes, *J. Biol. Chem. 273*, 31203−31208.
19. Rezaie, A. R., Cooper, S. T., Church, F. C., and Esmon, C. T. (1995) Protein C inhibitor is a potent inhibitor of the thrombin-thrombomodulin complex, *J. Biol. Chem. 270*, 25336−25339.
20. Rezaie, A. R., He, X., and Esmon, C. T. (1998) Thrombomodulin increases the rate of thrombin inhibition by BPTI, *Biochemistry 37*, 693−699.
21. Parry, M. A., Stone, S. R., Hofsteenge, J., and Jackman, M. P. (1993) Evidence for common structural changes in thrombin induced by active-site or exosite binding, *Biochem. J. 290*, 665−670.
22. Ye, J., Esmon, N. L., Esmon, C. T., and Johnson, A. E. (1991) The active site of thrombin is altered upon binding to thrombomodulin, *J. Biol. Chem. 266*, 23016−23021.
23. Mandell, J. G., Baerga-Ortiz, A., Akashi, S., Takio, K., and Komives, E. A. (2001) Solvent accessibility of the thrombin-thrombomodulin interface, *J. Mol. Biol. 306*, 575−589.
24. Ni, F., Konishi, Y., and Scheraga, H. A. (1990) Thrombin-bound conformation of the C-terminal fragments of hirudin determined by transferred nuclear Overhauser effects, *Biochemistry 29*, 4479−4489.
25. Mandell, J. G., Falick, A. M., and Komives, E. A. (1998) Measurement of amide hydrogen exchange by MALDI-TOF mass spectrometry, *Anal. Chem. 70*, 3987−3995.
26. Mandell, J. G., Falick, A. M., and Komives, E. A. (1998) Identification of protein−protein interfaces by decreased amide proton solvent accessibility, *Proc. Natl. Acad. Sci. U.S.A. 95*, 14705−14710.
27. Hughes, C. A., Mandell, J. G., Anand, G. S., Stock, A. M., and Komives, E. A. (2001) Phosphorylation causes subtle changes in solvent accessibility at the interdomain interface of methylesterase CheB, *J. Mol. Biol. 307*, 967−976.
28. Baerga-Ortiz, A., Rezaie, A. R., and Komives, E. A. (2000) Electrostatic dependence of the thrombin-thrombomodulin interaction, *J. Mol. Biol. 296*, 651−658.
29. Hoofnagle, A. N., Resing, K. A., Goldsmith, E. J., and Ahn, N. G. (2001) Changes in protein conformational mobility upon activation of extracellular regulated protein kinase-2 as detected by hydrogen exchange, *Proc. Natl. Acad. Sci. U.S.A. 98*, 956−961.
30. Anand, G. S., Hughes, C. A., Jones, J. M., Taylor, S. S., and Komives, E. A. (2002) Amide H/^{2}H exchange reveals communication between the cAMP and the catalytic subunit binding sites in the regulatory subunit of protein kinase A, *J. Mol. Biol. 323*, 377−386.
31. Hofsteenge, J., Braun, P. J., and Stone, S. R. (1988) Enzymatic properties of proteolytic derivatives of human alpha-thrombin, *Biochemistry 27*, 2144−2151.
32. Suel, G. M., Lockless, S. W., Wall, M. A., and Ranganathan, R. (2002) Evolutionarily conserved networks of residues mediate allosteric communication in proteins, *Nat. Struct. Biol. 10*, 59−68.

BI0499718